Oil Shale, 2018, Vol. 35, No. 3, pp. 279–289
doi: https://doi.org/10.3176/oil.2018.3.07
ISSN 0208-189X

LIQUEFACTION OF OIL SHALE IN SUPERCRITICAL ETHANOL

TIANHUA YANG[(a)], BING ZHOU[(a)], RUNDONG LI[(a)*], BINGSHUO LI[(b)], WENQI ZHANG[(a)], XINGPING KAI[(a)]

[(a)] Key Laboratory of Clean Energy of Liaoning, College of Energy and Environment, Shenyang Aerospace University, Shenyang 110136, China
[(b)] School of Environmental Science and Engineering, Tianjin University, Tianjin 300072, China

Abstract. *Oil shale was liquefied in supercritical ethanol in an autoclave. The effects of reaction temperature and residence time on the liquefaction of oil shale were studied. The optimum conditions for liquefaction were 360 °C and 210 min, which gave a shale oil yield of 18.15 wt%. According to Fourier transform infrared spectroscopy (FT-IR) and gas chromatography-mass spectrometry analysis (GS-MS), the main components of shale oil were alkanes and alcohols, accounting for about 39% of the total. Shale oil exhibited a high heating value of 37.72 MJ/kg with a water content of 0.4 wt% and a total acid number of 77.0 mg KOH/g oil.*

Keywords: *oil shale liquefaction, supercritical ethanol, reaction temperature, residence time.*

1. Introduction

The contradiction between oil supply and demand represents a problem for global energy requirements. Therefore, it is very important to look for an abundant substitute, and oil shale is one such source that may be the most ideal alternative. Oil shale is a sedimentary rock which contains combustible organic matter. It has been listed as an important resource to replace oil in the 21st century. Furthermore, it has been reported that the reserves of oil shale are about 10 trillion tons in the world, which is equivalent to 500 billion tons of shale oil. The reserves of oil shale in China are about 719.9 billion tons, which is equivalent to about 47.6 billion tons of shale oil, which is much higher than its proven oil reserves [1–3]. At present, oil shale is utilized in four major ways, including low-temperature carbonization to

* Corresponding author: e-mail *rdlee@163.com*

obtain shale oil, gasification to produce gas, manufacture of building materials, and burning directly as a fuel.

Sub-supercritical liquefaction is an efficient thermal conversion technology, which has been a hot topic in biomass and coal thermal conversion technology research in recent years. Ethanol is a renewable organic solvent and can provide active hydrogen in the liquefaction process. The reaction conditions utilizing supercritical ethanol are mild, and the requirement for costly equipment is minimal [4, 5]. Therefore, the study of liquefaction technology in sub-supercritical ethanol has been attracting significant attention recently. Xu and Donald [6] studied the liquefaction of peat in supercritical ethanol, and the results showed that the oxygen and nitrogen contents were significantly reduced in the liquefied oil. Tao et al. [7] investigated the liquefaction behavior of corn stalks in sub-supercritical ethanol. The results demonstrated that when the reaction temperature was 320 °C, the yield of heavy oil was 13.8% and that of the solid residue was 17.8%. The free radicals in ethanol promoted the reaction of cellulose present in corn stalks and inhibited the formation of more residues. Zheng et al. [8] studied the liquefaction of straw in supercritical ethanol. It was found that ethanol showed good performance in heat transfer and dissolution, and afforded a steady hydrogen supply. Moreover, the higher concentration of ethanol could effectively inhibit the formation of the residues and gases during liquefaction of the straw and significantly improved the yield of the liquefied oil. Zhou et al. [9] pointed out that the liquefied oil obtained by using either alcohols or water as solvent differed in composition. The composition of the liquefied oil obtained from alcohol was similar to that of biodiesel.

Reports on the liquefaction of oil shale in ethanol for shale oil production are rare. The purpose of this study was to elucidate the effects of various reaction conditions on the liquefaction of oil shale. It was expected that the results would help better understand the mechanism of oil shale liquefaction, which could provide a reference for the utilization of liquefied oil shale in the future.

2. Materials and methods

2.1. Materials and reagents

The oil shale samples were collected from Fushun, Liaoning Province, China. The samples were ground and passed through a 0.25 mm screen. Anhydrous ethanol (99.7%) was employed as the reactant and acetone (99.5%) was used as the washing solvent. Both ethanol and acetone were of analytical grade purity (Tianjin Kemiou Chemical Reagent Co., Ltd., China). All of the chemicals were commercially available and used as received without further purification. The results of proximate and ultimate analyses of oil shale are summarized in Table 1.

Table 1. Proximate and ultimate analyses of oil shale

Proximate analysis, %				Ultimate analysis, %				
M_{ad}	A_{ad}	V_{ad}	FC_{ad}	N	C	H	S	O[a]
1.81	79.25	17.58	1.35	1.01	12.09	2.53	0.52	2.79

[a] $O\% = 100 - (C + H + N + S + A_{ad} + M_{ad})\%$.

2.2. Liquefaction process and product separation

All the liquefaction experiments were carried out in an autoclave of 500 mL capacity. The autoclave was equipped with a magnetic stirrer to allow oil shale to mix well with ethanol. The autoclave was also equipped with a temperature controller with an accuracy of ±0.5 °C. During the experiment, the temperature and pressure data were recorded by computer.

For the liquefaction process, 20 g of oil shale and 200 mL of ethanol were added to the autoclave, which was then sealed and purged with N_2 to remove the air. The autoclave was heated to the desired temperature (280–360 °C) by an external jacket heater at a heating rate of 4 °C/min for desired residence times (30–270 min). Upon completion, the jacket was unloaded and the reactor was cooled to room temperature using a fan. The exhaust valve was opened to collect the gas. Next, the reactor was opened and the mixtures were poured out. Ethanol and acetone were used to clean the inner wall and pipeline to obtain the mixture of the organic liquid and the residue. The mixture was then filtered under vacuum to obtain the organic phase and the remaining solid. The organic phase was evaporated under vacuum at 80 °C to obtain shale oil. The solid was dried at 105 °C for 12 h and its yield was quantified.

2.3. Analytical methods

2.3.1. Physicochemical characteristics

The water content of shale oil was determined using the SYD-2122C Coulometric Karl Fischer titrator (Shanghai Changji, China), which follows the ASTM D6304-07 [10].

The total acid number (TAN) of shale oil was determined by the SYD-264B Automatic Total Acid Number tester (Shanghai, Changji), which follows the ASTM D664 protocol, together with the potentiometric titration method [11].

Elemental compositions (C, H, O, N) of oil shale and shale oil were determined by a CHONS elemental analyzer (EA3000, Italy).

The conversion of oil shale was described as follows:

$$\text{Conversion} = \frac{m_{\text{oil shale}} - m_{\text{residue}}}{m_{\text{oil shale}}} \times 100\% . \quad (1)$$

The yield of shale oil was obtained using the following equation:

$$\text{Yield}_{\text{oil}} = \frac{m_{\text{oil}}}{m_{\text{oil shale}}} \times 100\%. \quad (2)$$

The yield of residue was found by Equation (3) as follows:

$$\text{Yield}_{\text{residue}} = \frac{m_{\text{residue}}}{m_{\text{oil shale}}} \times 100\%, \quad (3)$$

The higher heating value (HHV) was calculated using the Boie formula (Eq. 4) [12]:

$$\text{HHV}(\text{MJ} \cdot \text{kg}^{-1}) = 0.3516\text{C} + 1.16225\text{H} - 0.1109\text{O} + 0.0628\text{N} + 0.10465\text{S}. \quad (4)$$

In the above equations, $m_{\text{oil shale}}$, m_{oil} and m_{residue} refer to the masses of oil shale, shale oil and residue, respectively; C, H, O, N and S refer to the mass fractions of the respective elements.

2.3.2. Fourier transform infrared spectroscopy

Fourier transform infrared spectroscopy (FT-IR) was performed on the Thermo Scientific Nicolet iS50 spectrometer (USA) to determine the functional groups in shale oil over the spectral range of 4000–500 cm^{-1} with a resolution of 4 cm^{-1}. A background scan was performed under ambient atmosphere prior to all measurements.

2.3.3. Gas chromatography-mass spectrometry

Shale oil was analyzed via gas chromatography-mass spectrometry (GC-MS) by using Shimadzu's GC/MS-QP5050 (Japan). Helium was used as the carrier gas at a flow rate of 20 mL/min and the split ratio was 1:36. A DB-1 column (30 m × 0.25 mm × 0.25 μm) was used for the separation. The oven isothermal program was set at 28 °C for 3 min, followed by heating to 180 °C at a rate of 5 °C/min and, subsequently, to 280 °C at 10 °C/min for 10 min. The volume of the injected sample was 1 μL and the scanned masses ranged from 20 to 500 amu in the electron ionization (70 eV) mode.

3. Results and discussion

3.1. Reaction temperature

The effect of reaction temperature on the yield of shale oil is shown in Figure 1. From the figure it can be seen that the reaction temperature was the main factor affecting the yield of shale oil. The temperature range of the experiment was 280–360 °C.

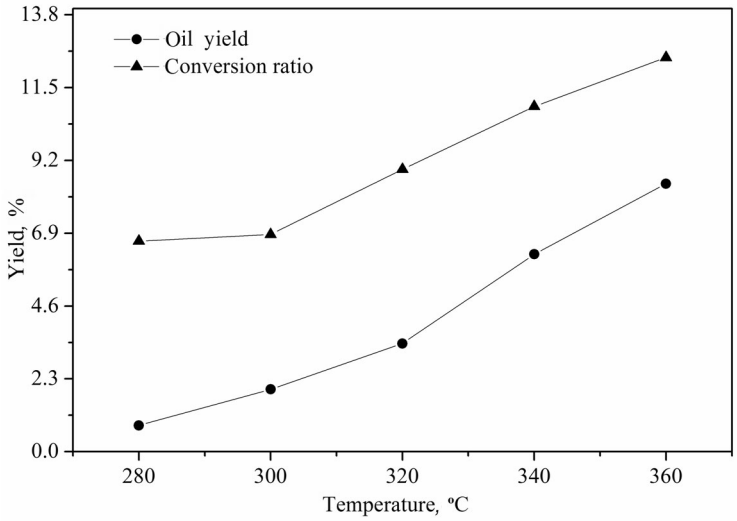

Fig. 1. Effect of reaction temperature on shale oil yield.

With the increase in liquefaction temperature, the shale oil yield and conversion ratio gradually increased. The shale oil yield increased from 0.83 to 8.47 wt% when the temperature was increased from 280 to 360 °C. The initial stage of oil shale decomposition was observed to take place at lower temperatures. The softening of kerogen and recombination of molecules produced asphalt and resulted in lower shale oil yield while the residue yield was high. With increase in the reaction temperature, the further decomposition of kerogen and cracking of bitumen contributed to production of shale oil and gas [13, 14]. With increasing temperature, the conversion ratio of oil shale increased gradually from 6.65 to 12.45 wt%. Furthermore, the residue yield decreased from 93.35 to 87.55 wt%, indicating a higher degree of the decomposition of oil shale. Therefore, the optimum liquefaction temperature was determined to be 360 °C.

3.2. Residence time

Residence time is also a key factor that affects the yield of shale oil. The effect of residence time on shale oil yield at 360 °C is illustrated in Figure 2. With increasing residence time, the yield of shale oil gradually increased and the maximum yield was 18.15 wt% at 210 min. As the residence time continued to increase, the yield of shale oil decreased. With shorter residence time, the primary reaction of the fractures and recombination of the cross-linking bonds in kerogen were incomplete. With increasing residence time, the decomposition of kerogen progressed further and the shale oil yield gradually increased to its maximum. With the further increase in the residence time, a secondary reaction of kerogen became predominant. In this

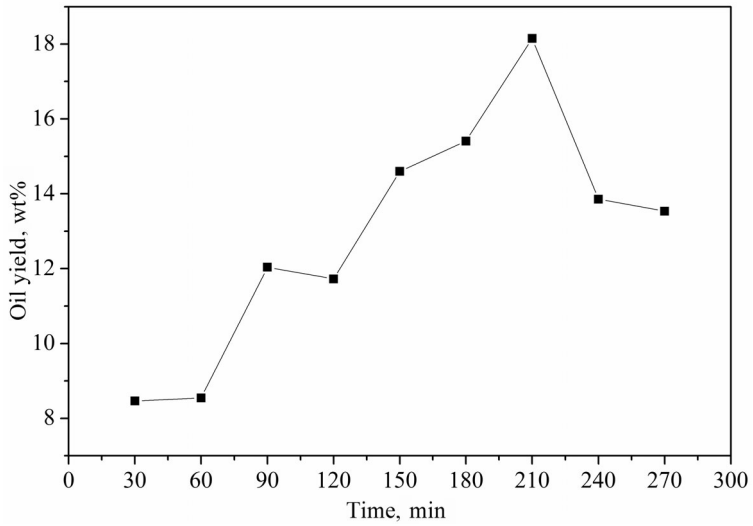

Fig. 2. Effect of residence time on shale oil yield.

reaction, the shale oil molecules underwent cleavage and polyreactions, while also releasing small molecules of gas, which reduced the yield of shale oil [15–17]. Thus, the experimental results showed that the optimum residence time was 210 min at a temperature of 360 °C.

3.3. Analysis of shale oil

3.3.1. FT-IR analysis

The distribution of main functional groups of shale oil was analyzed by FT-IR spectroscopy. The FT-IR spectrum of shale oil obtained under the optimized liquefaction conditions (360 °C, 210 min) is shown in Figure 3. FT-IR can provide information about the functional groups, the aliphatic and aromatic ring structures, and the aromatic organic composition of shale oil. The position and intensity of the absorption peaks depend on the number of functional groups of the compounds and the form and total amount of specific chemical bonds [18].

The absorbance peaks between 3650 and 3000 cm^{-1} were attributed to the –OH stretching vibrations. The detection signal of these peaks was wide and strong, indicating that alcohols and phenolic compounds were produced after liquefaction of oil shale. The peaks between 3000 and 2700 cm^{-1} were caused by the C–H stretching, bends and deformations in the methyl and methylene groups. This observation indicated the presence of aliphatic and alkyl aromatic compounds. A very small absorbance peak occurred in the region between 2500 and 2000 cm^{-1}, which was attributed to the stretching vibration of the alkynyl moiety. The absorbance peaks between 1700 and 1500 cm^{-1} were assigned to the C=O and C=C stretching vibrations. Thus, it

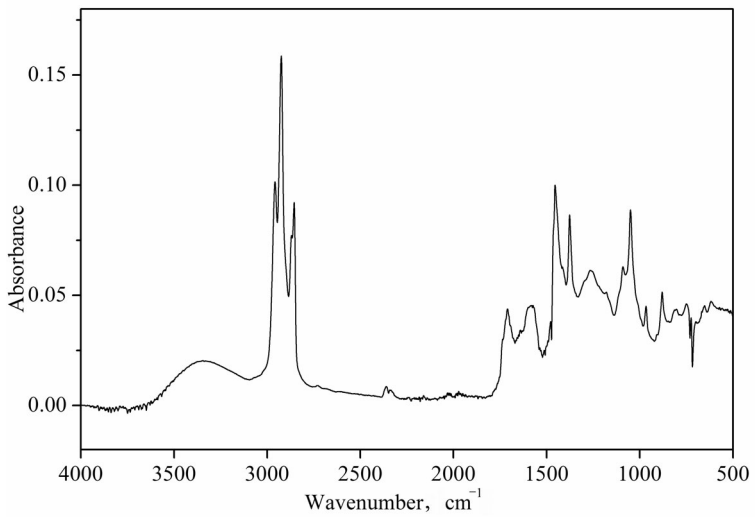

Fig. 3. Fourier transform infrared spectroscopy of shale oil.

was concluded that there were alkynes and olefins compounds in shale oil. The vibrational absorption peaks of the C–O group appeared at 1300 and 910 cm^{-1}, indicating that shale oil contained alcohols and ester compounds. The absorption peaks below 910 cm^{-1} could be attributed to the C–H vibrations in aromatic compounds and their derivatives. These results showed that shale oil contained alcohols, phenols, esters, ketones, olefins, carboxylic acids, aldehydes, and other compounds.

3.3.2. GC-MS analysis

The GC-MS analysis of shale oil was carried out under the optimum liquefaction conditions, at 360 °C and for 210 min. A total of 60 species were detected in shale oil, of which compounds with the relative content higher than 0.5% accounted for 59.97% of the total. Most of these species were identified as hydrocarbons and either chain or cyclic oxygen-containing compounds, with different mass fractions, from 2 to 44 carbon atoms. At the same time, the compounds contained the alcohol hydroxyl, aldehyde, carbonyl, carboxyl, ester and other functional groups (Fig. 4). The alkane content in shale oil was 30.38%. The species of alkanes and the distribution of carbon numbers are displayed in Table 2.

The second largest component was alcohols (8.77%), followed by esters, ketones, olefins, carboxylic acids and aldehydes. The compounds with the highest content were *n*-tridecane and *n*-octacosane. These two compounds may be obtained from the decomposition and polycondensation of kerogen in oil shale because kerogen typically contains a large number of aliphatic and aromatic compounds [19]. In addition, the main esters in shale oil were ethyl hexanoate and ethyl octanoate. The ketones were primarily aliphatic

ketones such as 2-octanone and 2-decanone. Furthermore, the heteroatomic compounds were mainly oxygenated. Also, nitrogen and chlorine compounds, such as 3-chlorooctane and 4-*n*-pentylpyridine, were present in small amounts.

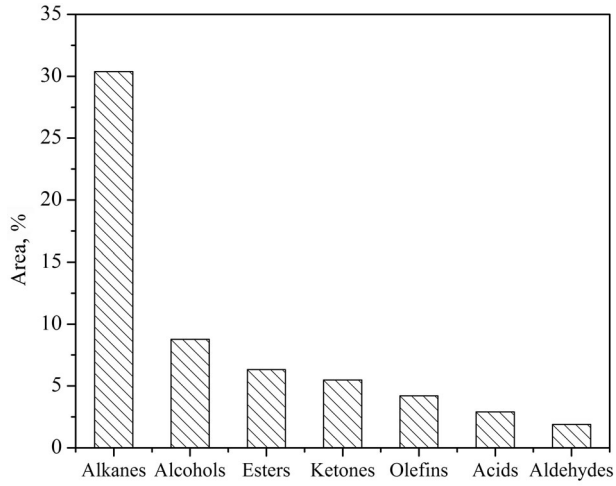

Fig. 4. Relative content of various substances in shale oil.

Table 2. GC-MS analysis of alkanes in shale oil

No	RT	Compound	Formula	Area, %
1	16.564	Cyclopropane, 1-heptyl-2-methyl	$C_{11}H_{22}$	0.68
2	18.794	Cyclohexane, pentyl-	$C_{11}H_{22}$	0.74
3	19.301	5-Ethyldecane	$C_{12}H_{26}$	1.03
4	19.458	Undecane, 3,7-dimethyl-	$C_{13}H_{28}$	0.54
5	19.646	2,6-Dimethyldecane	$C_{12}H_{26}$	2.42
6	19.943	Undecane, 3,4-dimethyl-	$C_{13}H_{28}$	0.78
7	20.097	3,8-Dimethyldecane	$C_{12}H_{26}$	1.11
8	21.054	Bicyclo[4.1.0]heptane, 7-pentyl-	$C_{12}H_{22}$	0.58
9	22.031	Cyclohexane, hexyl-	$C_{12}H_{24}$	0.64
10	22.644	Octane, 4-methyl-	C_9H_{20}	0.81
11	22.959	Undecane, 3-ethyl-	$C_{13}H_{28}$	0.6
12	23.101	Dodecane, 3-methyl-	$C_{13}H_{28}$	0.67
13	23.809	Undecane, 6-ethyl-	$C_{13}H_{28}$	1.02
14	23.945	Tridecane	$C_{13}H_{28}$	3.98
15	25.091	Undecane, 3,5-dimethyl-	$C_{13}H_{28}$	1.26
16	25.286	Undecane, 4-ethyl-	$C_{13}H_{28}$	0.74
17	25.469	5-Methyltridecane	$C_{14}H_{30}$	0.56
18	25.786	Dodecane, 2,6,11-trimethyl-	$C_{15}H_{32}$	0.85
19	25.925	3,8-Dimethyldecane	$C_{12}H_{26}$	0.68
20	31.799	Pentadecane	$C_{15}H_{32}$	3.21
21	35.981	Eicosane	$C_{20}H_{42}$	1.85
22	40.037	Pentadecane, 8-heptyl-	$C_{22}H_{46}$	0.91
23	43.007	Octacosane	$C_{28}H_{58}$	3.38
24	44.841	Dotriacontane	$C_{32}H_{66}$	0.71
25	45.89	Tetratetracontane	$C_{44}H_{90}$	0.63

3.3.3. Characteristics of shale oil

The physicochemical characteristics of shale oil are important reference indicators for the design, evaluation and selection of the conveying device and the shaping of the treatment device. Furthermore, these parameters have a direct impact on the application scope and utilization efficiency of shale oil. Therefore, the water content, TAN and HHV of shale oil were determined and ultimate analysis was performed under the optimal liquefaction conditions. These results are presented in Table 3.

Table 3. Characteristics of shale oil

	Characteristic	Shale oil
Physicochemical characteristics	Water content, wt%	0.4
	TAN, mg KOH/g oil	77.0
	HHV, MJ/kg	37.72
Ultimate analysis	C, %	77.01
	H, %	9.96
	O, % [a]	10.27
	N, %	2.06
	S, %	0.70

[a] Calculated by difference.

Water content can directly affect the HHV and flame temperature of shale oil. The water content of shale oil was found to be 0.4 wt%. Furthermore, the shale oil was acidic and its TAN was 77.0 mg KOH/g oil. The HHV of shale oil (37.72 MJ/kg) was higher than that of bio-oil derived from lingocellulosic biomass [4]. The contents of C and H were also relatively high; the H/C atomic ratio was 1.55 and the O/C atomic ratio was 0.10.

4. Conclusions

The reaction temperature and residence time during the liquefaction process of oil shale had a significant effect on the yield of shale oil. The optimum operating conditions were the following: liquefaction temperature 360 °C and residence time 210 min. Fourier transform infrared spectroscopy and gas chromatography-mass spectrometry analyses showed that the main components of shale oil were alkanes and alcohols, which accounted for about 39% of the total. The higher heating value of shale oil was 37.72 MJ/kg and its water content was 0.4 wt%. This study demonstrated that shale oil could be obtained when oil shale was liquefied using supercritical ethanol, which provided a new method for oil shale utilization.

Acknowledgments

This work was supported by the National Natural Science Foundation of China (No. 51576135) and the Aeronautical Science Foundation of China (No. 2015ZB54006).

REFERENCES

1. Qi, Z. L., Li, Y. L., Wang, C. S., Sun, T., Zhang, J. H. Organic geochemistry of the Paleocene-Eocene oil shales of the Gongjue Formation, Nangqian Basin, east-central Tibetan Plateau. *Oil Shale*, 2017, **34**(1), 1–14.
2. Ma, L., Yin, X. Y., Sun, H., Fu, B. S. Present status of oil shale resource utilization in the world and its development prospects. *Global Geology*, 2012, **31**(4), 772–777 (in Chinese with English abstract).
3. Hou, J. L., Ma, Y., Li, S. Y., Teng, J. S. Development and utilization of oil shale worldwide. *Chemical Industry and Engineering Progress*, 2015, **34**(5), 1183–1190 (in Chinese with English abstract).
4. Li, R. D., Li, B. S., Yang, T. H., Kai, X. P., Wang, W. D., Jie, Y. F., Zhang, Y., Chen, G. Y. Sub-supercritical liquefaction of rice stalk for the production of bio-oil: Effect of solvents. *Bioresource Technol.*, 2015, **198**, 94–100.
5. Liu, H. M., Xie, X. A., Ding, N. P., Liu, H. B., Huang, L. Y. Liquefaction reaction pathway and mechanism of cornstalk in sub- and supercritical ethanol. *Transactions of the CSAE*, 2010, **26**(6), 277–282 (in Chinese with English abstract).
6. Xu, C. B., Donald, J. Upgrading peat to gas and liquid fuels in supercritical water with catalysts. *Fuel*, 2012, **102**, 16–25.
7. Tao, H. X., Xie, X. A., Zheng, C. Y., Tang, C. Z., Zhan, X. Q. Liquefaction of cornstalk cellulose in sub-/supercritical ethanol. *Journal of Northwest A & F University (Nat. Sci. Ed.)*, 2014, **42**(1), 196–204 (in Chinese with English abstract).
8. Zheng, C. Y., Xie, X. A., Tao, H. X., Zheng, L. S., Li, Y. Depolymerization of stalk cellulose during its liquefaction in sub- and supercritical ethanol. *Journal of Fuel Chemistry and Technology*, 2012, **40**(5), 526–532 (in Chinese with English abstract).
9. Zhou, D., Zhang, S. C., Fu, H. B., Chen, J. M. Liquefaction of macroalgae *Enteromorpha prolifera* in sub-/supercritical alcohols: Direct production of ester compounds. *Energ. Fuel.*, 2012, **26**(4), 2342–2351.
10. ASTM D6304-07. *Standard Test Method for Determination of Water in Petroleum Products, Lubricating Oils, and Additives by Coulometric Karl Fischer Titration*, 2007.
11. ASTM D664. *Standard Test Method for Acid Number of Petroleum Products by Potentiometric Titration*, 2006.
12. Yang, T. H., Jie, Y. F., Li, B. S., Kai, X. P., Yan, Z., Li, R. D. Catalytic hydrodeoxygenation of crude bio-oil over an unsupported bimetallic dispersed catalyst in supercritical ethanol. *Fuel Process. Technol.*, 2016, **148**, 19–27.
13. Fedyaeva, O. N., Antipenko, V. R., Dumov, D. Yu., Kruglyakova, T. V., Vostrikov, A. A. Non-isothermal conversion of the Kashpir sulfur-rich oil shale in a supercritical water flow. *J. Supercrit. Fluid.*, 2016, **109**, 157–165.
14. Li, Y., Wu, D., Han, G., Liu, J. Pyrolysis characteristic and production analysis

of Fushun oil shale. *Journal of Liaoning Technical University (Natural Science)*, 2014, **33**(12), 1613–1616 (in Chinese with English abstract).
15. Toor, S. S., Rosendahl, L., Rudolf, A. Hydrothermal liquefaction of biomass: A review of subcritical water technologies. *Energy*, 2011, **36**(5), 2328–2342.
16. Zhong, C. L., Wei, X. M. A comparative experimental study on the liquefaction of wood. *Energy*, 2004, **29**(11), 1731–1741.
17. Li, R. D., Zhang, Y., Li, B. S., Liu, H. X., Kai, X. P., Yan, Z., Yang, T. H. Hydrothermal catalytic liquefaction of corn stalk for preparation of bio-oil. *Journal of Fuel Chemistry and Technology*, 2016, **44**(1), 69–75 (in Chinese with English abstract).
18. Xie, F. F., Wang, Z., Song, W. L., Lin, W. G. FTIR analysis of oil shales from Huadian Jilin and their pyrolysates. *Spectroscopy and Spectral Analysis*, 2011, **31**(1), 91–94 (in Chinese with English abstract).
19. Song, W. N., Dong, Y. L., Zhou, G. J., Ding, H. X, Li, Z. Research summarization of structure-constitute and application of oil shale. *Journal of Heilongjiang Hydraulic Engineering*, 2010, **37**(3), 70–73 (in Chinese with English abstract).

Presented by J. Soone and Yue Ma
Received July 28, 2017